J|A|C|S
ARTICLES
Published on Web 00/00/0000

The Mechanism of the Self-Initiated Thermal Polymerization of Styrene. Theoretical Solution of a Classic Problem

Kelli S. Khuong,[†] Walter H. Jones,[†] William A. Pryor,[‡] and K. N. Houk*,[†]

Contribution from the Department of Chemistry and Biochemistry, University of California, Los Angeles, California 90095-1569, and Department of Chemistry, Louisiana State University, Baton Rouge, Louisiana 70803-1804

Received August 25, 2004; E-mail: houk@chem.ucla.edu

Abstract: The Mayo and Flory mechanisms for the self-initiation of styrene polymerization were explored with B3LYP and BPW91 density functional calculations. The Diels−Alder dimer (**AH**) is the key intermediate, and the lowest energy pathway for **AH** formation is a stepwise mechanism via a gauche/sickle (**•M$_2$•Gs**) or gauche/U-shaped (**•M$_2$•Gu**) diradical. Ring closure of the 1,4-diradical to diphenylcyclobutane (**DCB**) is predicted to have a lower barrier than ring closure to **AH**. Dynamic effects are likely to play an important role in determining the rate of **AH** versus **DCB** formation. Hydrogen transfer from **AH** to styrene to generate two monoradical species is predicted to be a reasonable process that initiates monoradical polymerization.

Introduction

Polystyrene is among the most important synthetic polymers, used in everything from home insulation products and drinking cups to plastic cutlery and those "peanuts" that spill out when a fragile package arrives in the mail. The control of polymerization is of great commercial significance. Whereas the controlled thermal polymerization produces the highest molecular weight in radical initiated polystyrene,[1] undesirable spontaneous polymerizations can clog styrene production facilities. Purified styrene polymerizes at a rate of 0.1% per hour at 60 °C and 2% per hour at 100 °C.[2]

Several mechanisms for the spontaneous thermal polymerization were proposed two-thirds of a century ago, but there is no consensus as to the correct mechanism.[3] The contenders are the Mayo mechanism and the Flory mechanism, depicted in Figure 1. According to the Mayo mechanism,[4] radical initiation proceeds by a Diels−Alder dimerization of styrene. Molecule-assisted homolysis[1,5] between the dimer (**AH**) and a third styrene generates the monoradical initiators **A•** and **HM•** that initiate polymerization. Flory proposes that styrene dimerizes to form a singlet 1,4-diradical (**•M$_2$•**).[6] A third styrene abstracts a hydrogen atom from the diradical to generate monoradical initiators capable of starting the chain polymerization process. Alternatively, the diradical itself may be capable of initiating polymerization. Finally, there is a connection between the Mayo and Flory proposals: the diradical may actually ring-close to form either 1,2-diphenylcyclobutane (**DCB**), a species that is inactive to polymerization, or the **AH** dimer, in which case the Diels−Alder cycloadduct is formed in a stepwise process and then can transfer hydrogen and initiate polymerization.

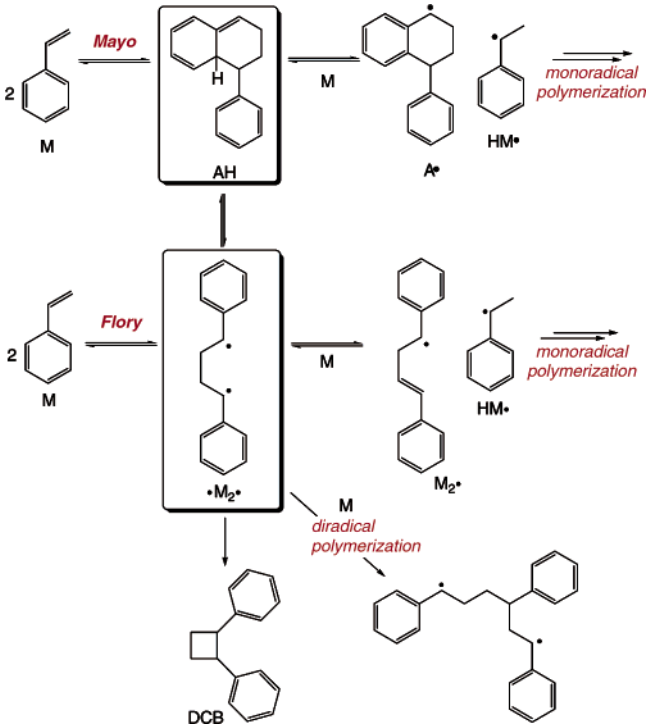

Figure 1. Mayo and Flory mechanisms.

We have undertaken an investigation of these mechanisms using modern computational methods. B3LYP,[7] a hybrid density

[†] University of California, Los Angeles.
[‡] Louisiana State University.

(1) Pryor, W. A. Radical Polymerizations. *Free Radicals*; McGraw-Hill: New York, 1966; pp 117−129, 237−239. Molecular weight is inversely proportional to square root of initiator concentration.
(2) Rubens, L. C.; Boyer, R. F. The Polymerization of Styrene. In *Styrene*; Boundy, R. H., Boyer, R. F., Eds.; ACS Monograph 115; Reinhold: New York, 1952; pp 215−288.
(3) An excellent review on the subject of spontaneous polymerization of styrene: Pryor, W. A.; Lasswell, L. D. *Adv. Free-Radical Chem.* **1975**, *5*, 27−99.
(4) (a) Mayo, F. R. *J. Am. Chem. Soc.* **1968**, *90*, 1289−1295. (b) Mayo, F. R. *J. Am. Chem. Soc.* **1953**, *75*, 6133−6141.
(5) (a) Pryor, W. A. *Petroleum Prepr.* **1980**, *25*, 12−18. (b) Pryor, W. A.; Coco, J. H.; Daly, W. H.; Houk, K. N. *J. Am. Chem. Soc.* **1974**, *96*, 5591−5593.
(6) Flory, P. J. *J. Am. Chem. Soc.* **1937**, *59*, 241−253.

10.1021/ja0448667 CCC: $30.25

functional method, accurately reproduces activation barriers and reaction energies for concerted pericyclic reactions[8] as well as for competing stepwise processes.[9,10] In some cases, however, pure generalized gradient DFT methods such as BLYP[7] or BPW91[11] outperform hybrid DFT methods for the exploration of singlet diradical surfaces.[12] In view of these results, we have applied both B3LYP and BPW91 to the study of styrene self-polymerization: the mechanism for formation of key intermediates **AH** and **•M$_2$•**, the subsequent generation of active monoradical species, and the competing self-termination via **DCB** formation. We have also used model systems to examine the processes of monoradical versus diradical polymerization, chain transfer, and termination.

Background

Numerous experimental studies have tackled the question of whether the Diels−Alder dimer **AH** or the diradical **•M$_2$•** is the essential intermediate in the self-initiation process. Most studies support the formation of **A•** and **HM•** as the monoradical initiators, but the diradical **•M$_2$•** has not been unequivocally ruled out as playing a role in the initiation process.

Thermal polymerization of styrene produces both polymer and a complex mixture of dimers and trimers whose composition is dependent on the reaction conditions.[4] In the absence of initiators or radical inhibitors, *trans*- and *cis*-1,2-diphenylcyclobutane are the major dimeric products formed in a 2:1 ratio, with minor amounts of 1-phenyltetralin (**PhT**), 1,3-diphenylcyclobutane, and 1-phenyl-1,2-dihydronaphthalene (**PhN**).[13] The presence of I_2 in the reaction catalyzes formation of **PhT**[4] at the expense of cyclobutane formation,[14] whereas the presence of aromatic nitro compounds leads to inhibition of polymerization and increases the formation of **PhN**.[4] The presence of the dimers indicates the formation of both the 1,4-diradical as well as the **AH** dimer but does not provide direct evidence for the mechanism of polymer initiation.

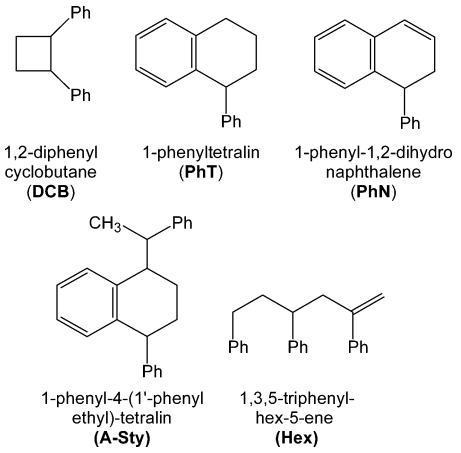

Table 1. Relative Amounts of Dimer, Trimer, and Polymer Formed during Self-Initiated Styrene Polymeriztion

dimer	trimer	polymer	conditions	ref
8.4×10^{-3} mol % 3.0×10^{-3} mol % **PhT** 1.8×10^{-3} mol % c**DCB** 3.6×10^{-3} mol % t**DCB**	5.0×10^{-2} mol %	3.8×10^{-3} mol % (MW 500 000)	85 °C 31 hr	13
0.7% mostly **DCB** 3:1 trans to cis	95.5% 32.7% **Hex** 62.8% **A-Sty**		130−150 °C 50% conv	15
0.023% 2:1 *trans* to *cis*-**DCB**	0.082%		137 °C 10% conv	16
0.1 to 0.3 wt % 80−90% **DCB**	0.67 wt % 95% **A-Sty**		137, 180 °C 97% conv	17

The major trimers are 1,3,5-triphenylhex-5-ene (**Hex**) and stereoisomers of 1-phenyl-4-(1′-phenylethyl)-tetralin (**A-Sty**). The formation of **A-Sty** has implications for the initiation mechanism. One reasonable mechanism involves reaction of **AH** and **M** to generate a caged radical pair, **A•/HM•**. Radical combination generates **A-Sty**, diffusion out of the cage leads to the initiating species **A•** and **HM•**, and disproportionation produces dimer **PhT**. Alternatively, **A-Sty** could be formed in a single step by an ene reaction of **AH** and styrene (Figure 2).

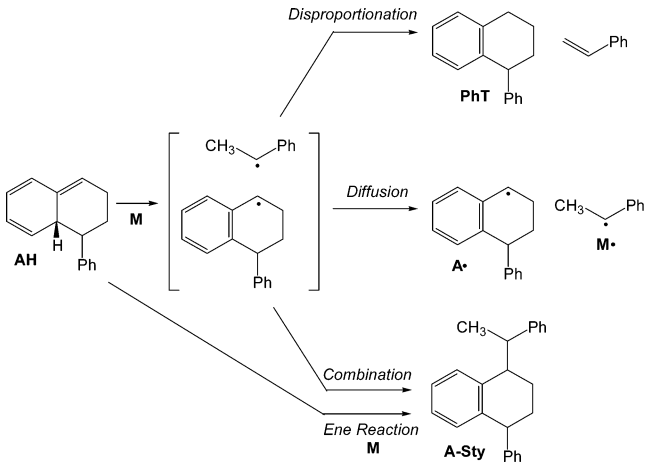

Figure 2. Postulated reaction mechanism that explains the reactivity of the **AH** intermediate. Reaction of **AH** with styrene monomer generates a caged radical pair that can then undergo further reactions.

The relative amounts of dimer, trimer, and polymer, listed in Table 1, give several clues to the mechanism of the self-initiation process. First, the amount of products derived from **AH** (dimer **PhT** and trimer **A-Sty**) significantly outweighs the amount of **DCB**. Second, the relative amounts of **PhT**, **A-Sty**, and polymer give a rough indication of the relative rates of disproportionation, combination, and diffusion.[3] On the basis of Brown's results,[13] the rates of disproportionation and diffusion out of the cage are roughly the same, and the rate of combination is about 10 times faster. This is qualitatively consistent with Kirchner and Buchholz's results that indicate the activation

(7) (a) Becke, A. D. *J. Chem. Phys.* **1993**, *98*, 5648−5652. (b) Lee, C.; Yang, W.; Parr, R. G. *Phys. Rev. B* **1988**, *37*, 785.
(8) Guner, V.; Khuong, K. S.; Leach, A. G.; Lee, P.; Bartberger, M. D.; Houk, K. N. *J. Phys. Chem. A* **2003**, *107*, 11445−11459.
(9) (a) Khuong, K. S.; Houk, K. N. *J. Am. Chem. Soc.* **2003**, *125*, 14867−14883. (b) Suhrada, C. P.; Houk, K. N. *J. Am. Chem. Soc.* **2002**, *124*, 8796−8797. (c) Nendel, M.; Sperling, D.; Wiest, O.; Houk, K. N. *J. Org. Chem.* **2000**, *65*, 3259−3268. (d) Beno, B. R.; Wilsey, S.; Houk, K. N. *J. Am. Chem. Soc.* **1999**, *121*, 4816−4826. (e) Houk, K. N.; Nendel, M.; Wiest, O.; Storer, J. W. *J. Am. Chem. Soc.* **1997**, *19*, 10545−10546. (f) Houk, K. N.; Beno, B. R.; Nendel, M.; Black, K.; Yoo, H. Y.; Wilsey, S.; Lee, J. *Theochem* **1997**, *398*−*399*, 169−179.
(10) Gräfenstein, J.; Hjerpe, A. M.; Kraka, E.; Cremer, D. *J. Phys. Chem. A* **2000**, *104*, 1748−1761.
(11) Burke, K.; Perdew, J. P.; Wang, W. In *Electronic Density Functional Theory: Recent Progress and New Directions*; Dobsin, J. F., Vignale, G., Das, M. P., Eds.; Plenum: New York, 1998.
(12) (a) Winkler, M.; Sander, W. *J. Phys. Chem. A* **2001**, *105*, 10422−10432. (b) Staroverov, V. N.; Davidson, E. R. *J. Am. Chem. Soc.* **2000**, *122*, 7377−7385.
(13) Brown, W. G. *Makromol. Chem.* **1969**, *128*, 130−136.
(14) Dodson, R. M.; Zielske, A. G. *J. Org. Chem.* **1967**, *32*, 28−31.

energy for **A-Sty** formation is 20.5 kcal/mol while the activation energy of initiation is 9 kcal/mol higher.[16]

Attempts to trap the initiating species have been moderately successful. Chong et al. reported that the propagation of styrene polymerization was effectively retarded with $FeCl_3$ in DMF without any change in the normal course of the reaction.[18] Use of $FeCl_3$ as a trapping agent did not affect the distribution and rate of formation of dimers and trimers. Oligostyrenes **1-Cl** and **2-Cl** were isolated and characterized by ^{1}H NMR and UV, suggesting that monoradicals **HM•** and **A•** were both initiators.

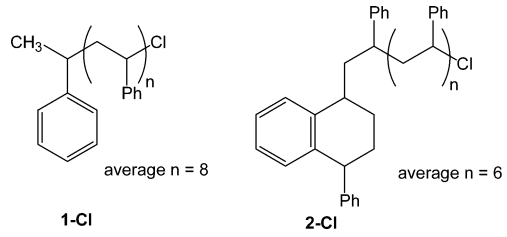

Nitroxides have also been used as trapping agents, and structures analogous to oligomers **1-Cl** and **2-Cl** have been identified.[19,20] Unlike $FeCl_3$, which does not interfere with the rate of initiation, nitroxides are consumed at rates significantly higher than the rate of styrene initiation.

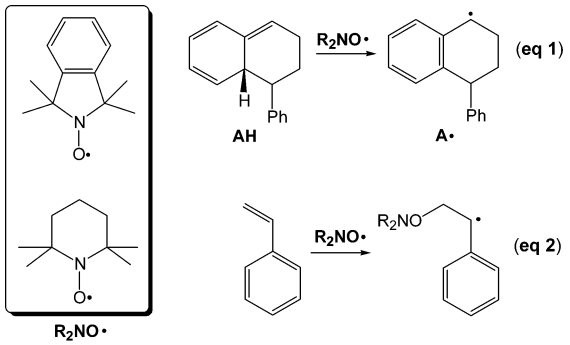

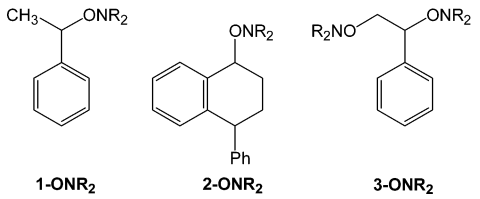

Nitroxides can abstract hydrogen from the Mayo dimer **AH** (eq 1) and can add directly to the double bond of styrene (eq 2), catalyzing the formation of **2-ONR$_2$** and **3-ONR$_2$**. Additionally, hydroxylamines, **R$_2$NOH**, can transfer hydrogen to styrene to catalyze the formation of **1-ONR$_2$**. The 1,4-diradical intermediate is not trapped in these experiments, but 1,2-diphenylcyclobutanes are still present in the product mixture.[19]

Buzanowski et al. probed the nature of the initiating species with the hypothesis that the 1,4-diradical should be immune to acid catalysis but the Mayo dimer **AH** would be quickly aromatized to inactive dimer **PhT** in the presence of acid.[21] Increasing acid strength or concentration resulted in retarded rates of polymerization and increased molecular weights, supporting the role of the **AH** in the polymerization.

Several studies have used kinetic isotope effects as a probe for the initiation step. Use of styrene-β,β-d_2 gave an inverse KIE of 0.78−0.88[22] and rules out the following initiating step:

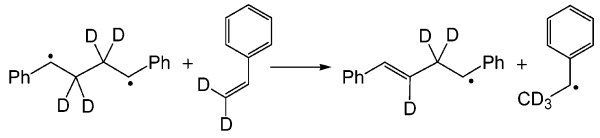

Replacing the *ortho*-hydrogens of styrene with deuterium labels resulted in a modest normal KIE, suggesting that the *ortho*-H(D) is transferred to another molecule of styrene in the rate-determining initiating step.[22] This interpretation is consistent with the formation of monoradicals **A•** and **HM•** and with the third-order initiation reported by Mayo for styrene polymerization in bromobenzene[4b] and independently verified by Hiatt and Bartlett for a styrene/ethyl thioglycolate mixture.[23]

Thermolysis of 3,6-diphenyl-3,4,5,6-tetrahydropyridazines (**4** and **5**) was used as an alternative method for generation of the 1,4-diradical **•M$_2$•** and study of its reactivity.

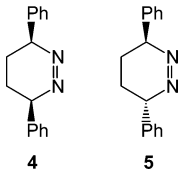

Thermolysis of **4** produces *trans*-**DCB** and *cis*-**DCB** in a 1:2 ratio, thermolysis of **5** gives a 23:1 ratio, and styrene polymerization gives a 2:1 ratio.[24] These differing ratios of *trans*- to *cis*-**DCB** indicate that the initial conformation, or vibrational energy distribution, of the diradical **•M$_2$•** formed from **4** or **5** is different than that formed by tail-to-tail dimerization of styrene. Nonetheless, the experiments fail to provide support for the Flory mechanism because no other styrene dimers such as **PhT** or **PhN** were isolated from the product mixture, and thermolysis of **4** or **5** in styrene failed to give appreciable rates of polymerization.

Photochemical generation of the 1,4-diradical from compounds **6** and **7** differs from the thermolysis of **4** and **5** in that 1-phenyltetralin (**PhT**) is an observed dimeric product in addition to **DCB** and styrene.[25] The yield of **PhT** was highly dependent on the diradical precursor and on the light source (either lamp or laser). The authors concluded that the conformation of the short-lived diradical should influence its propensity

(15) Kurze, V. J.; Stein, D. J.; Šimák, P.; Kaiser, R. *Angew. Makromol. Chem.* **1970**, *12*, 25−41.
(16) Kirchner, V. K.; Buchholz, K. *Angew. Makromol. Chem.* **1970**, *13*, 127−138.
(17) Kirchner, K.; Riederle, K. *Angew. Makromol. Chem.* **1983**, *111*, 1−16.
(18) Chong, Y. K.; Rizzardo, E.; Solomon, D. H. *J. Am. Chem. Soc.* **1983**, *105*, 7761−7762.
(19) Moad, G.; Rizzardo, E.; Solomon, D. H. *Polym. Bull.* **1982**, *6*, 589−593.
(20) Devonport, W.; Michalak, L.; Malmström, E.; Mate, M.; Kurdi, B.; Hawker, C. J.; Barclay, G. G.; Sinta, R. *Macromolecules* **1997**, *30*, 1929−1934.
(21) Buzanowski, W. C.; Graham, J. D.; Priddy, D. B.; Shero, E. *Polymer* **1992**, *33*, 3055−3059.
(22) (a) Pryor, W. A.; Henderson, R. W.; Patsiga, R. A.; Carroll, N. *J. Am. Chem. Soc.* **1966**, *88*, 1199−1205. (b) Kirchner, K. *Makromol. Chem.* **1966**, *96*, 179−186. (c) Kopecky, K. R.; Evani, S. *Can. J. Chem.* **1969**, *47*, 4049−4058. (d) Henderson, R. W.; Pryor, W. A. *Int. J. Chem. Kinet.* **1972**, *4*, 325−330.
(23) Hiatt, R. R.; Bartlett, P. D. *J. Am. Chem. Soc.* **1959**, *81*, 1149−1154.
(24) (a) Kopecky, K. R.; Evani, S. *Can. J. Chem.* **1969**, *47*, 4041−4048. (b) Kopecky, K. R.; Soler, J. *Can. J. Chem.* **1974**, *52*, 2111−2118.
(25) Miranda, M. A.; Font-Sanchis, E.; Pérez-Prieto, J.; Scaiano, J. C. *J. Org. Chem.* **1999**, *64*, 7842−7845.

to fragment, cyclize to **DCB**, or cyclize to **AH**.[25] *cis*-**DCB**, *trans*-**DCB**, **PhT**, and 2-phenyltetralin are dimers typically observed during photopolymerization of styrene,[26] but no **AH** derivatives (e.g., phenyltetralin) have been observed upon photolysis of diphenylcyclobutanes.[27]

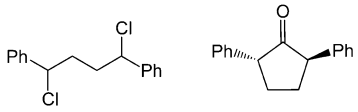

6 **7**

The thermal rates of initiation, propagation, chain transfer, and termination have been measured and are listed in Table 2. Because the measured rate of initiation R_i corresponds to a complex rate equation that depends on the rates of several elementary steps, it is not directly comparable to a single computed activation barrier. However, the experimental values can serve as a guide for whether the calculated activation barriers are reasonable.

Table 2. Rate Constants for Self-Initiated Styrene Polymerization Measured by Viscometry at 25 °C[28] [a]

	k	E_a	log A	$\Delta H^{\ddagger}$	$\Delta G^{\ddagger}$	$\Delta S^{\ddagger}$
initiation	1.32×10^{-15}	37 ± 2	10.09	36.4	37.7	−14.3
propagation	18.7	6.5 ± 1	6.01	5.9	15.7	−33.0
transfer	6.68×10^{-4}	14.2 ± 1	7.18	13.6	21.8	−27.7
termination	2.79×10^{6}	2.8 ± 1	8.19	2.2	8.7	−23.0

[a] Rate constants and log A values are given in $M^{-1}s^{-1}$; E_a, $\Delta H^{\ddagger}$, $\Delta G^{\ddagger}$ in kcal/mol; and $\Delta S^{\ddagger}$ in eu.

The experimental evidence strongly points to the intermediacy of the **AH** dimer, but the questions still remain: what is the mechanism for formation of **AH**? Is the 1,4-diradical an obligatory intermediate, or do concerted [4+2] and diradical [2+2] cycloadditions compete?

Computational Methodology

Geometry optimizations were performed with B3LYP/6-31G* and BPW91/6-31G* as implemented in Gaussian 98.[29] Diradicals and transition structures leading to diradicals were treated with unrestricted B3LYP and BPW91 in cases when the HOMO−LUMO mixing in the initial guess led to unrestricted wave functions that were more stable than the corresponding restricted wave functions. All minima and transition structures were characterized by their vibrational frequencies. Reported energies are relative enthalpies (ΔH_{298K}) and relative free energies (ΔG_{298K}) and include unscaled zero-point energy corrections and thermal corrections to 298 K. $\langle S^2 \rangle$ values of the singlet diradical species range from 0.1 to 1.1, indicating varying degrees of spin contamination. Spin correction[30,31] was carried out on the diradical species to estimate pure singlet UB3LYP energies. The UBPW91 diradical species were not spin corrected.

Results and Discussion

The organization of the Results section of this paper is as follows. First, the concerted cycloadditions of styrene are described. Next, the stepwise diradical pathways are discussed, with close attention given to the various conformations and lifetime of the styrene 1,4-diradical formed from dimerization of styrene. Third, the generation of monoradical species is explored, and monoradical versus diradical propagation is compared. Fourth, the role of dynamics on the outcome of the styrene dimerization is discussed in the context of both computational and experimental results. Finally, the processes of chain transfer and disproportionation are examined. For those readers who are less interested in the computational details describing the behavior of 1,4-diradicals, we recommend skipping to the section titled "Monoradical and diradical initiators."

Scheme 1

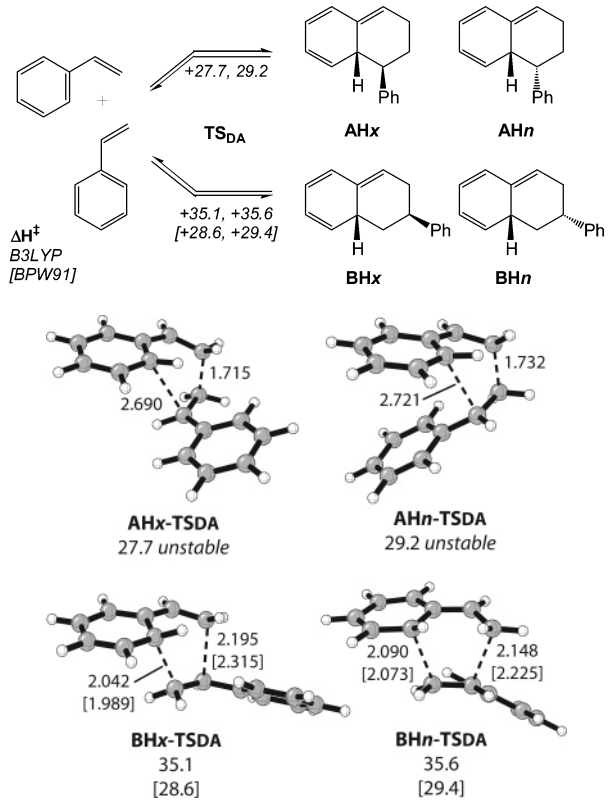

Figure 3. Diels−Alder TSs for the dimerization of styrene. B3LYP and BPW91 [in brackets] enthalpies in kcal/mol. Bond lengths are given in Å.

Concerted Cyclization To Form Diels−Alder Adducts AH and BH. Two molecules of styrene can dimerize to give four possible Diels−Alder adducts (Scheme 1). There are two **AH** dimers, classified here as **AHx** and **AHn**, where x and n are abbreviations for exo and endo.[32] The opposite regiochemistry

(26) (a) Li, T.; Padia, A. B.; Hall, H. K., Jr. *Macromolecules* **1990**, *23*, 3899−3904. (b) Kauffmann, H. F. *Mackromol. Chem.* **1979**, *180*, 2649−2663, 2665−2680, 2681−2693, 2695−2705.
(27) Jones, G., II; Chow, V. L. *J. Org. Chem.* **1974**, *39*, 1447−1448.
(28) Bamford, C. H.; Dewar, M. J. S. *Proc. R. Soc. (London)* **1948**, *A192*, 309−328.
(29) Frisch, M. J.; Trucks, G. W.; Schlegel, H. B.; Scuseria, G. E.; Robb, M. A.; Cheeseman, J. R.; Zakrzewski, V. G.; Montgomery, J. A., Jr.; Stratmann, R. E.; Burant, J. C.; Dapprich, S.; Millam, J. M.; Daniels, A. D.; Kudin, K. N.; Strain, M. C.; Farkas, O.; Tomasi, J.; Barone, V.; Cossi, M.; Cammi, R.; Mennucci, B.; Pomelli, C.; Adamo, C.; Clifford, S.; Ochterski, J.; Petersson, G. A.; Ayala, P. Y.; Cui, Q.; Morokuma, K.; Malick, D. K.; Rabuck, A. D.; Raghavachari, K.; Foresman, J. B.; Cioslowski, J.; Ortiz, J. V.; Baboul, A. G.; Stefanov, B. B.; Liu, G.; Liashenko, A.; Piskorz, P.; Komaromi, I.; Gomperts, R.; Martin, R. L.; Fox, D. J.; Keith, T.; Al-Laham, M. A.; Peng, C. Y.; Nanayakkara, A.; Challacombe, M.; Gill, P. M. W.; Johnson, B.; Chen, W.; Wong, M. W.; Andres, J. L.; Gonzalez, C.; Head-Gordon, M.; Replogle, E. S.; Pople, J. A. *Gaussian 98*, Revision A.9; Gaussian, Inc.: Pittsburgh, PA, 1998.
(30) (a) Yamaguchi, K.; Jensen, F.; Dorigo, A.; Houk, K. N. *Chem. Phys. Lett.* **1988**, *149*, 537−542. (b) Yamanaka, S.; Kawakami, T.; Nagao, H.; Yamaguchi, K. *Chem. Phys. Lett.* **1994**, *231*, 25−33.
(31) Potential problems with spin projected DFT are discussed: Wittbrodt, J. M.; Schlegel, H. B. *J. Chem. Phys.* **1996**, *105*, 6574−6577.

Table 3. Enthalpies (ΔH_{298K}) and Free Energies (ΔG_{298K}) in kcal/mol for Transition Structures and Intermediates Potentially Involved in the Self-Initiation of Styrene, Relative to Styrene

	ΔH_{298K}		ΔG_{298K}	
	B3LYP (with spin correction)	BPW91	B3LYP (with spin correction)	BPW91
Concerted Cycloaddition to AH and BH				
AHx−TS_{DA}	27.7[b]	*a*	43.1[b]	*a*
AHn−TS_{DA}	29.2[b]	*a*	44.3[b]	*a*
BHx−TS_{DA}	35.1	28.6	50.2	43.3
BHn−TS_{DA}	35.6	29.4	50.9	44.4
Stepwise Cycloaddition to AH and DCB and Diradical Intermediates				
TS_1 (At)	25.4 (21.7)	19.8	38.1 (34.4)	32.5
TS_1 (Ac)	25.2 (21.6)	19.7	38.3 (34.7)	32.7
TS_1 (Gs)	25.2 (22.1)	19.6	38.9 (35.7)	33.2
TS_1 (Gu)	26.3 (23.1)	21.2	39.5 (36.4)	34.5
TS_1 (Gw)	27.3 (23.4)	22.0	39.8 (35.9)	34.5
$^{\bullet}M_2^{\bullet}$ (At)	21.0 (19.5)	19.5	33.3 (31.7)	31.6
$^{\bullet}M_2^{\bullet}$ (Ac)	21.0 (19.5)	19.6	33.8 (32.3)	32.3
$^{\bullet}M_2^{\bullet}$ (Gs)	21.4 (19.8)	19.9	34.0 (32.4)	32.9
$^{\bullet}M_2^{\bullet}$ (Gu)	22.0 (20.3)	20.7	34.4 (32.8)	33.3
$^{\bullet}M_2^{\bullet}$ (Gw)	22.0 (21.4)	21.0	33.6 (33.0)	32.3
TS_{2x}	26.4 (23.2)	20.2	42.0 (38.9)	35.8
TS_{2n}	27.6 (24.3)	21.8	42.9 (39.6)	36.3
TS_{cisDCB}	24.0 (19.8)	21.8	38.0 (33.8)	36.1
$TS_{transDCB}$	22.3 (18.0)	19.8	36.3 (32.0)	32.8
$TS_{transDCB'}$	25.1 (21.1)	23.3	39.0 (35.1)	37.1
Styrene Dimers AH, BH, DCB				
AHx	−0.3	−2.6	15.5	13.1
AHn	2.0	−0.3	17.9	15.6
BHx	0.5	−2.0	16.5	14.0
BHn	−0.6	−2.9	15.0	12.5
cis-DCB	−7.4	−9.6	7.3	5.0
trans-DCB	−11.2	−13.5	3.7	1.1
Monoradical Initiators (H Abstraction)				
AHx + M: TS_{Habs}	23.9 (23.5)	15.0	52.3 (51.9)	43.4
AHn + M: TS_{Habs}	23.0 (22.0)	13.9	50.7 (49.7)	41.6
AHx + M: TS_{Ene}	19.6	11.6	49.1	40.9
AHn + M: TS_{Ene}	19.2	11.2	49.2	40.7
$A^{\bullet}$ + $HM^{\bullet}$ initiators	1.7	−0.3	16.2	14.0
$^{\bullet}M_2^{\bullet}$ + M: TS_{Habs}	42.5 (42.1)	35.3	65.7 (65.4)	58.4
$M_2^{\bullet}$ + $HM^{\bullet}$ initiators	17.9	16.8	28.6	27.1
Styrene Trimer				
cis-A-Sty	−44.4	−44.4	−14.8	−14.6
trans-A-Sty	−43.4	−45.4	−13.5	−15.9
Monoradical Propagation				
$HM^{\bullet}$ + M: TS_{mono}	+7.7	+6.0	+20.1	+18.3
Diradical Propagation				
$^{\bullet}M_2^{\bullet}$ + M: TS_{dirad}	+7.3 (+8.1)	+6.3	+19.9 (+20.3)	+18.4
Chain Transfer				
AHx + $HM^{\bullet}$: TS_{tr}	+9.2	+6.8	+22.2	+19.4
AHn + $HM^{\bullet}$: TS_{tr}	+6.0	+3.4	+18.0	+15.1
Disproportionation				
$HM^{\bullet}$ + $HM^{\bullet}$: TS_{disp}	+2.9 (−1.1)		+15.9 (+12.0)	

[a] Concerted Diels−Alder transition structure could not be located with RBPW91/6-31G*. [b] Restricted wave function is unstable.

leads to formation of the **BH** dimers, **BHx** and **BHn**. The enthalpies and free energies of the concerted transition structures and resulting products are listed in Table 3.

Most striking is the prediction that Diels−Alder transition structures **AHx−TS_{DA}** and **AHn−TS_{DA}** are not stationary points on the potential energy surface. Although RB3LYP locates such structures, the restricted wave functions are unstable, indicating that unrestricted wave functions provide a better description of the electronic structures of the highly asynchronous optimized geometries (Figure 3). Reoptimization with UB3LYP generates diradical transition structures **TS_{2x}** and **TS_{2n}** (discussed in the next section). RBPW91 does not locate concerted **AH** transition structures; it actually locates **TS_{2x}** and **TS_{2n}** and describes these diradical transition structures with a closed-shell wave function (discussed in next section).

In contrast, both RB3LYP and RBPW91 locate the concerted transition structures for formation of the **BH** isomers. These TSs are more synchronous: the forming σ-bonds differ in length by only 0.1−0.2 Å and resemble typical Diels−Alder transition

(32) (a) Kauffmann, H. F.; Olaj, O. F.; Breitenbach, J. W. *Makromol. Chem.* **1976**, *177*, 939−945. (b) Olaj, O. F.; Kauffmann, J. F.; Breitenbach, J. W. *Makromol. Chem.* **1977**, *178*, 2707−2717. These two references report that time-dependent UV absorption of polymerizing styrene gives evidence for the formation of both the exo and the endo **AH** dimers. The authors conclude that the exo and endo isomers have different stationary concentrations.

Scheme 2

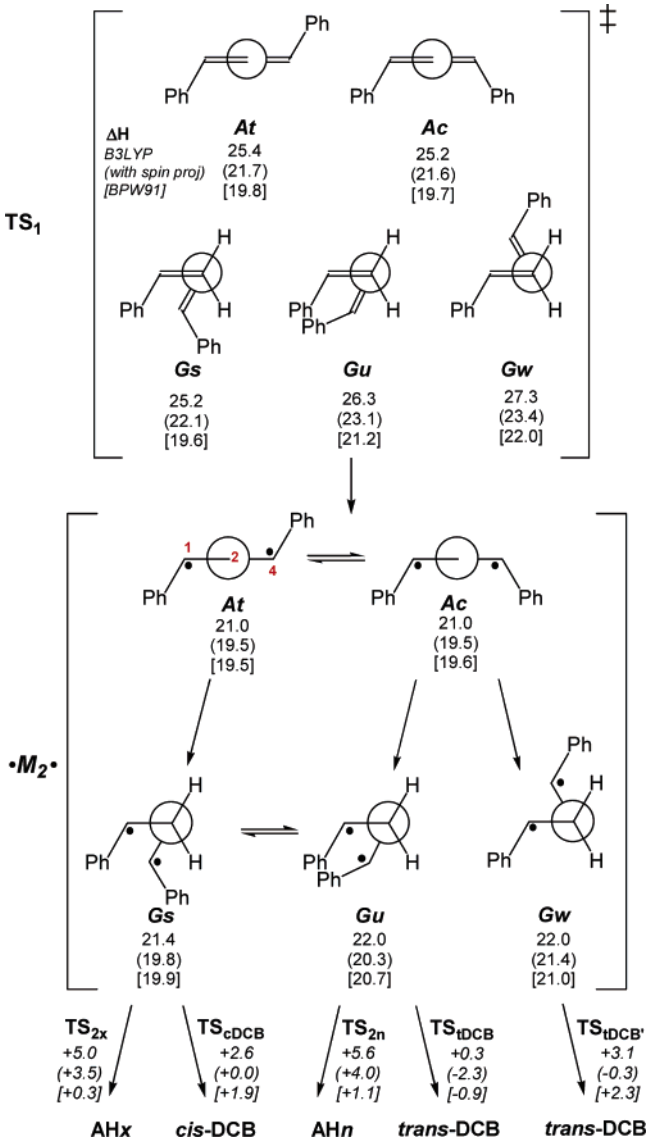

structures (Figure 3). RB3LYP predicts **BHx**−**TS$_{DA}$** and **BHn**−**TS$_{DA}$** to have enthalpies of 35.1 and 35.6, respectively, while RBPW91 predicts the enthalpies to be 4−5 kcal/mol lower. The free energies of activation are significantly higher than the relative enthalpies because of unfavorable activation entropies characteristic of bimolecular pericyclic reactions ($\Delta S^{\ddagger}_{298K}$ values range from −50.6 to −51.7 eu).

The results on the concerted transition structures imply that the Diels−Alder adducts **AHx** and **AHn** are not formed by a typical closed-shell cycloaddition but arise from stepwise cycloadditions involving highly stabilized diradicals. Interestingly, the activation energy of 25 kcal/mol is essentially the same as the concerted cycloaddition of butadiene and ethylene.[8]

Stepwise Cyclization To Form AH and DCB. The diradical **TS$_1$** corresponds to tail-to-tail bond formation and generation of the 1,4-diradical **•M$_2$•** (top of Scheme 2). Diradical bond formation can occur in five distinct conformations, referred to as **At** (anti-trans), **Ac** (anti-cis), **Gs** (gauche-sickle), **Gu** (gauche-U), and **Gw** (gauche-W). The first letter, either A or G, refers to the dihedral angle about the forming σ-bond. The second letter refers to the orientation of the phenyl groups with respect

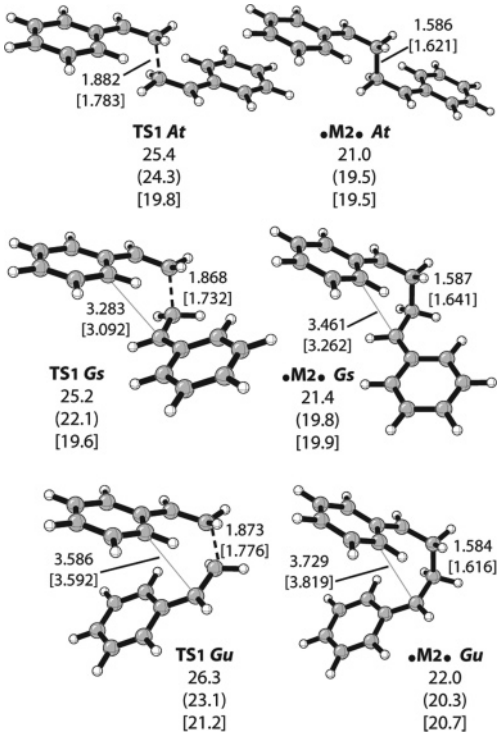

Figure 4. Diradical TSs and intermediates potentially involved in the stepwise formation of dimers. B3LYP, B3LYP with spin projection (in parentheses), and BPW91 [in brackets] enthalpies in kcal/mol. Bond lengths are given in Å.

to each other: trans, cis, sickle-shaped, U-shaped, or W-shaped. Of the five possible conformations for **TS$_1$**, **At**, **Ac**, and **Gs** have the most favorable enthalpies, while **Gu** and **Gw** have enthalpies that are 1−2 kcal/mol higher. A Boltzmann distribution based on the **TS$_1$** B3LYP enthalpies indicates that **At**, **Ac**, and **Gs** account for ∼95% of the 1,4-diradicals formed. When the free energies are used instead, the **At** and **Ac** account for ∼80% and **Gs** becomes less significant at 12%. Representative structures are shown in Figure 4.

The initially formed 1,4-diradical intermediates can also be described as **At**, **Ac**, **Gs**, **Gu**, and **Gw** conformers. Both UB3LYP and UBPW91 predict that the five **•M$_2$•** conformations shown in Scheme 2 all lie within 1.0−1.5 kcal/mol of each other. Rotations about the newly formed C2−C3 σ-bond have barriers of ∼2 kcal/mol and interconvert **At**/**Gs** and **Ac**/**Gu**/**Gw**.

Rotations about the C1−C2 bond or (alternatively the C3−C4 bond) cost very little energy and interconvert **At**/**Ac**, **Gs**/**Gu**, and **Gs**/**Gw**. Model calculations shown in Figure 5 indicate that C1−C2 dihedral angles of 90−270° differ in energy by less than 0.1 kcal/mol. Such low rotational barriers are typical of 6-fold potentials that lack steric repulsion.[33] From 270 to 0 to 90°, steric repulsion due to A1,3 strain becomes important, and the energy increases dramatically.

The primary difference in the UB3LYP and UBPW91 descriptions of the 1,4-diradical intermediates is that UB3LYP predicts **•M$_2$•** to lie in a deeper well (higher barriers to revert to styrene or to close to either **AH** or **DCB**) than predicted by UBPW91 (lower barriers to revert to styrene or to close to either **AH** or **DCB**). As discussed in the background section, the ratio of *cis*-**DCB** to *trans*-**DCB** is highly dependent on the method

(33) Sears, T. J.; Johnson, P. M.; Jin, P.; Oatis, S. *J. Chem. Phys.* **1996**, *104*, 781−792.

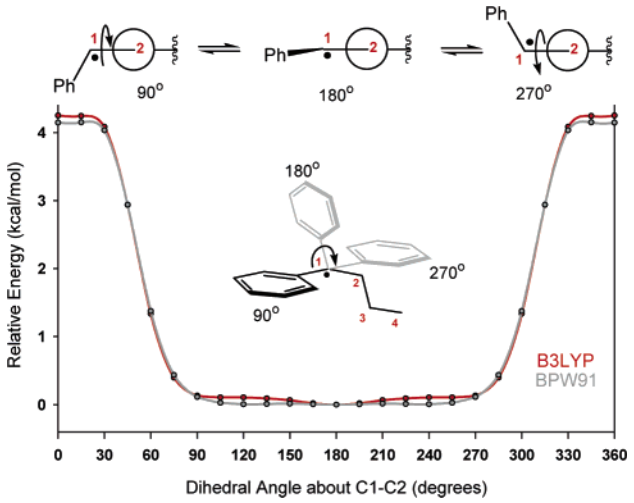

Figure 5. Model for the C1−C2 rotational potential in the **•M$_2$•** diradical. Conformations between 90 and 270° differ in energy by less than 0.1 kcal/mol and are thermally accessible.

of generating the 1,4-diradical. This implies that the lifetime of **•M$_2$•** is too short for complete equilibration among the various possible conformations.

As shown in Scheme 2, the gauche-type diradicals are the reactive conformers leading to styrene dimers via formation of a second σ-bond. The **•M$_2$•Gs** can form either **AHx** or *cis*-**DCB**, the **•M$_2$•Gu** can form either **AHn** or *trans*-**DCB**, and the **•M$_2$•Gw** can form only *trans*-**DCB**. This discussion will first focus on the characteristics of **TS$_{2x}$** and **TS$_{2n}$** and then on the characteristics of **TS$_{cDCB}$** and **TS$_{tDCB}$**.

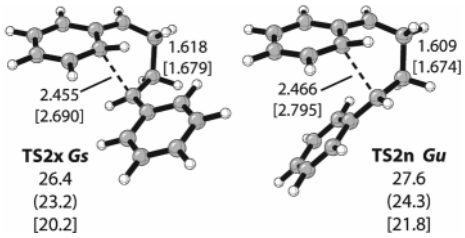

Figure 6. TSs for the ring closure of **•M$_2$•** to **AHx** and **AHn**. B3LYP, B3LYP with spin projection (in parentheses), and BPW91 [in brackets] enthalpies in kcal/mol. Bond lengths are given in Å.

TS$_{2x}$ and **TS$_{2n}$** correspond to the stepwise formation of the exo and endo Diels−Alder adducts (Figure 6). Figure 7a is a plot of the reaction coordinate describing conversion of **•M$_2$•Gs** (no bond B) to **AHx** (fully formed bond B) and is useful for illustrating several key features of these transition structures. First, UB3LYP predicts that the barrier to form **AHx** from the diradical is ∼5 kcal/mol, whereas UBPW91 predicts this barrier to be significantly lower, <1 kcal/mol. Second, B3LYP predicts that **TS$_{2x}$** occurs when bond B is 2.455 Å, which is located before the functional switches from the unrestricted to the restricted regime which occurs when bond B is ∼2.40 Å; consequently, the diradical transition structure **TS$_{2x}$** must be located with unrestricted B3LYP. On the other hand, BPW91 switches from the unrestricted to the restricted regime much earlier, when bond B is still ∼2.9 Å such that the diradical transition structure **TS$_{2x}$** is treated as a closed-shell structure with $\langle S^2 \rangle = 0$. As pointed out by Grafenstein et al.,[10] restricted hybrid density functionals such as B3LYP are characteristically less stable with respect to unrestricted solutions than GGA functionals such as BPW91.[34]

Scheme 3

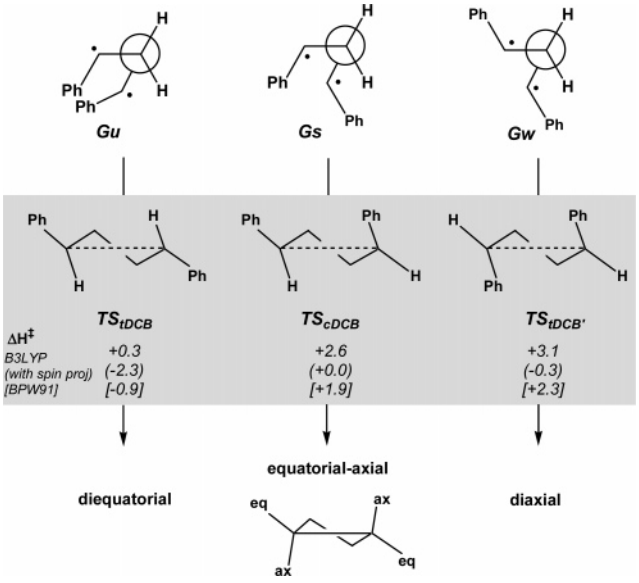

Third, a common feature of the B3LYP and BPW91 reaction coordinates is that bond A shows a cooperative lengthening and subsequent shortening as bond B is forming (Figure 7a, shaded triangles). This implies that **TS$_{2x}$** benefits from some vestiges of aromatic character[35] even though the cycloaddition proceeds by a stepwise [4+2] mechanism; stretching of bond A leads to some cyclic delocalization in the transition structure.

TS$_{2n}$ has characteristics similar to **TS$_{2x}$**. The relative enthalpy of **TS$_{2n}$** is slightly higher than that of **TS$_{2x}$** because of increased steric interactions between the two phenyl rings. In the exo Diels−Alder product, the remaining phenyl ring is in a pseudoequatorial position, whereas in the endo product the phenyl ring is in a pseudoaxial position.

The overall process, **TS$_1$** followed by either **TS$_{cDCB}$** or **TS$_{tDCB}$**, corresponds to a stepwise [2+2] cycloaddition (Figure 8). Figure 7b is a plot of the reaction coordinate describing conversion of **•M$_2$•Gs** (no bond C) to *cis*-**DCB** (fully formed bond C). As was observed in Figure 7a, BPW91 predicts a smaller barrier and flatter surface than B3LYP, and as a result, the forming cyclobutane bond (bond C) is longer in the BPW91 **TS$_{cDCB}$** than in the analogous B3LYP **TS$_{cDCB}$**. Of additional interest is that the stepwise [2+2] cycloaddition also demonstrates a cooperative effect of bond A as bond C is forming. In this case, the opposite effect is observed: bond A contracts and subsequently lengthens (Figure 7b, shaded triangles). **TS$_{cDCB}$** benefits by minimizing any electron delocalization, thus minimizing any vestiges of antiaromatic character. The fluctuation in the length of bond A is 10 times smaller for closure to *cis*-**DCB** (0.025 Å) than for closure to **AHx** (0.25 Å).

It is not obvious from the simple Newman projections of **•M$_2$•Gs**, **•M$_2$•Gu**, and **•M$_2$•Gw** why **TS$_{tDCB}$** is lower in enthalpy than **TS$_{tDCB'}$**. A side-view of the three transition structures leading to **DCB** dimers provides a clearer depiction of the steric and electronic factors involved in the formation of a cyclobutane ring (Scheme 3). As shown in the idealized representations of

(34) Hybrid DFT methods include a portion of exact HF exchange which leads to larger instability because HF is always less stable than DFT. Also see ref 7 and ref 12b.
(35) Leach, A. G.; Catak, S.; Houk, K. N. *Chem. Eur. J.* **2002**, *8*, 1290−1299.

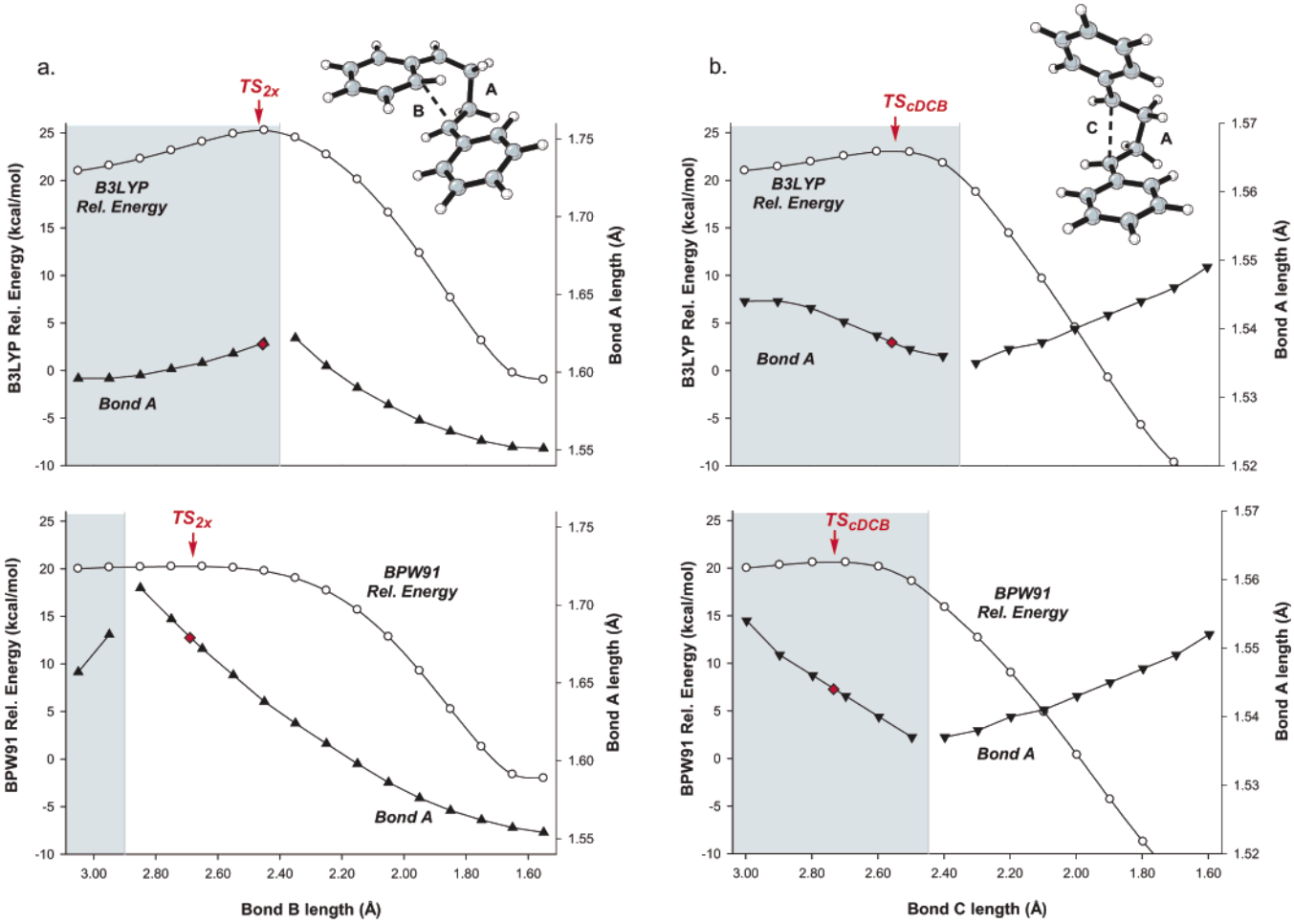

Figure 7. (a) B3LYP and BPW91 reaction coordinates for conversion of the diradical **•M$_2$•Gs** to the **AHx** adduct as bond B is formed. Relative energy (ZPE exclusive) and length of bond A are plotted as a function of length of bond B. (b) B3LYP and BPW91 reaction coordinates for conversion of the diradical **•M$_2$•Gs** to the *cis*-**DCB** adduct as bond C is formed. Relative energy (ZPE exclusive) and length of bond A are plotted as a function of length of bond C. The shaded portion of the reaction coordinate corresponds to the unrestricted DFT regime and unshaded to restricted DFT.

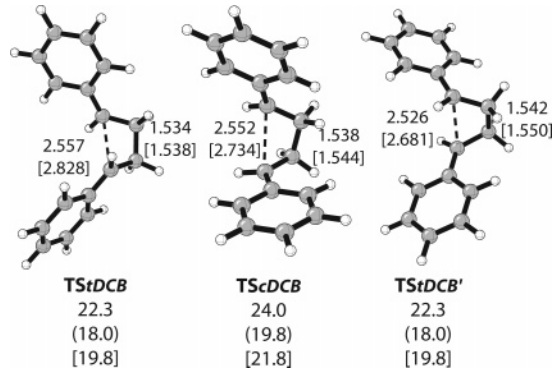

Figure 8. TSs for the ring closure of **•M$_2$•** to **DCB**. B3LYP, B3LYP with spin projection (in parentheses), and BPW91 [in brackets] enthalpies in kcal/mol. Bond lengths are given in Å.

the transition structures, **TS$_{tDCB}$** is lowest in enthalpy because it has two equatorial phenyl groups whereas **TS$_{tDCB'}$** is highest in enthalpy with two axial phenyl groups. Like the transition structures for ring closure of tetramethylene, the **TS$_{DCB}$** geometries show poor overlap of the carbons in the forming σ-bond.[36]

UB3LYP predicts that **•M$_2$•Gs** produces *cis*-**DCB** significantly faster than it produces **AHx**, and similarly, **•M$_2$•Gu** produces *trans*-**DCB** significantly faster than it produces **AHn** (Scheme 2). UBPW91, on the other hand, predicts that in some cases the **DCB** dimer is formed more slowly than the corresponding **AH** dimer. Because the thermolysis of azo compounds **4** and **5** and *cis*-**DCB** produced no isolable **AH** derivatives, it appears that UB3LYP has better agreement than UBPW91 with the experimental results involving the 1,4-diradical. In addition, activation parameters for the formation of both *cis*-**DCB** and *trans*-**DCB** and decomposition of *cis*-**DCB** have been measured experimentally (Table 4). The UB3LYP activation enthalpies closely match the experimental values, whereas both spin-corrected UB3LYP and UBPW91 predict activation enthalpies that are too low.

Finally, despite ring strain, the **DCB** dimers are approximately 10 kcal/mol more stable than the **AH** and **BH** dimers (Table 3) because two aromatic rings are maintained in the former. Consequently, cyclobutane adducts will not form Diels−Alder adducts upon equilibration.

Monoradical and Diradical Initiators. A key step in the spontaneous polymerization of styrene is the generation of radical initiators capable of adding to a styrene monomer. Scheme 4 highlights two processes that could potentially contribute to the formation of monoradical species.

(36) Doubleday, C., Jr. *J. Am. Chem. Soc.* **1993**, *115*, 11968−11983.

Table 4. Experimental Kinetic Parameters Measured for the Formation and Disappearance of *cis*- and *trans*-DCB

	experimental						calculated $\Delta H^{\ddagger}_{298K}$		
	ref	T (°C)	rate const (M^{-1} s^{-1})	E_a (kcal/mol)	log A (M^{-1} s^{-1})	$\Delta H,^{\ddagger}$ (kcal/mol)	B3LYP (kcal/mol)	spin corrected (kcal/ mol)	BPW 91 (kcal/mol)
2M → DCB	16	137	1.02×10^{-7}	25.9	6.8	25.1	25.4[a]	21.7	19.8
2M → DCB	17	137,180		28.0		27.1			
			(s^{-1})		(s^{-1})				
cis-DCB → M + *trans*-DCB	16	169	3.83×10^{-6}	39 ± 3	13.9	38.1			
cis-DCB → 2M	27	200	5.2×10^{5}	35.8	12.3	34.9	32.8[b]	29.1	29.4
cis-DCB → *trans*-DCB	27	200	2.4×10^{5}	35.6	11.8	34.7	31.4[c]	27.2	31.4

[a] Corresponds to enthalpy difference between styrene and **TS_1At**. [b]Corresponds to enthalpy difference between *cis*-**DCB** and **TS_1At**. [c]Corresponds to enthalpy difference between *cis*-**DCB** and **TS_{cisDCB}**.

Scheme 4

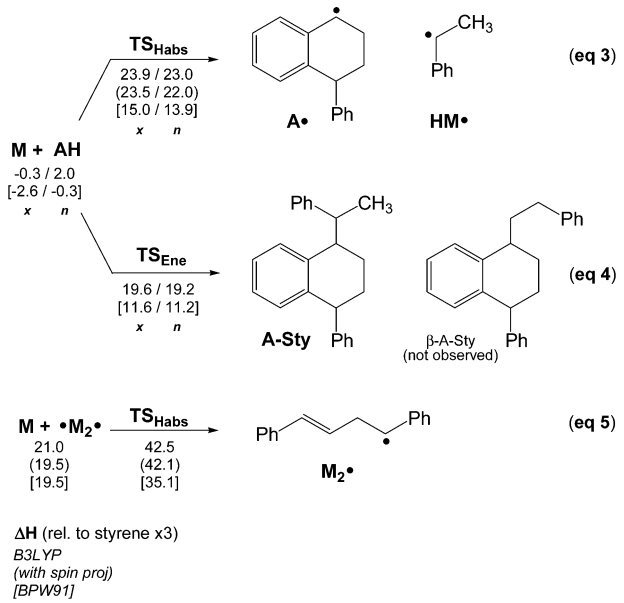

In eqs 3 and 5, styrene abstracts a hydrogen atom from either **AH** or **•M$_2$•** to generate phenylethyl radical **HM•** and another monoradical species capable of initiating the chain polymerization (Figure 9). B3LYP barriers for hydrogen abstraction are systematically 9 kcal/mol higher than the BPW91 barriers; however, both methods predict that abstraction from the **AH** cycloadducts is favored by 15−22 kcal/mol over abstraction from the 1,4-diradical. Likewise, the resulting monoradical **A•** is ∼17 kcal/mol more stable than **M$_2$•**. Another factor that casts doubt on the importance of eq 5 is that hydrogen abstraction from **•M$_2$•** would be significantly slower than ring closure to either **AH** or **DCB**. The computational prediction that hydrogen abstraction from **AH** is much more likely than from **•M$_2$•** is entirely consistent with the experimental KIE studies that indicate an *ortho*-deuterium and not a β-deuterium is transferred during the rate-determining step.[22]

An ene reaction between **AH** and styrene is one mechanism postulated for the formation of trimer **A-Sty** (eq 4). Kirchner and Buchholz report the activation energy for **A-Sty** formation as 20.5 kcal/mol (100−152 °C),[16] which is significantly lower than the measured activation energy of initiation of 37 kcal/mol.[28] For this reason, Kirchner and Buchholz propose the ene mechanism to be reasonable. Other authors, such as Pryor and Lasswell,[3] suggest that **A-Sty** is formed by both the ene reaction and by combination of monoradicals **A•** and **HM•**. Finally, Buzanowski et al. concluded that the ene reaction is not a viable pathway because FMO calculations predict that the major ene

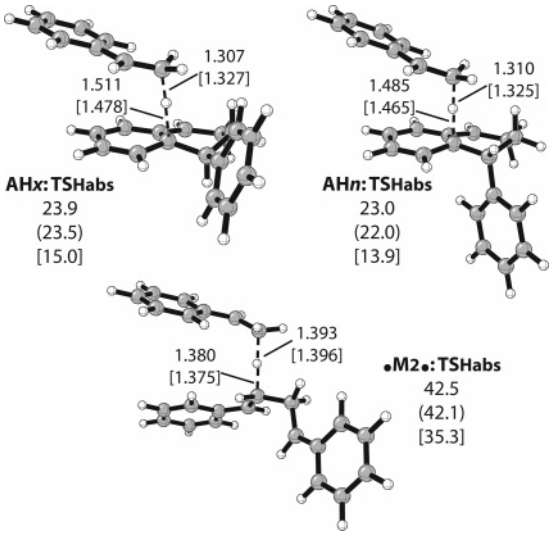

Figure 9. TSs for styrene hydrogen abstraction from **AH** or **•M$_2$•**. B3LYP, B3LYP with spin projection (in parentheses), and BPW91 [in brackets] enthalpies in kcal/mol. Bond lengths are given in Å.

product would be the β-phenethyl derivative which is not observed experimentally.[21]

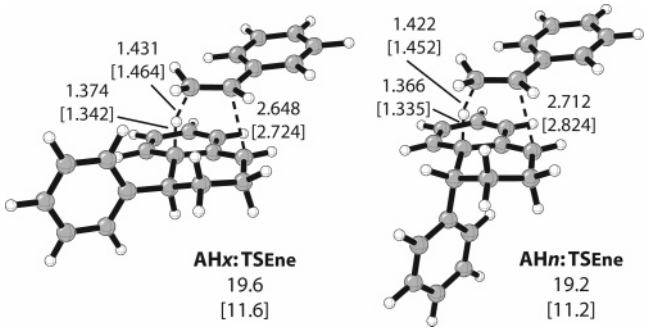

Figure 10. TSs for ene reaction between **AH** and styrene. B3LYP and BPW91 [in brackets] enthalpies in kcal/mol. Bond lengths are given in Å.

The calculated ene transition structures are shown in Figure 10. The ene reaction of **AHx** plus styrene has an activation enthalpy of 19.6 kcal/mol, which is 4.3 kcal/mol lower than the barrier for hydrogen abstraction. Similarly, the ene reaction involving **AHn** has an activation enthalpy of 19.2, which is 3.8 kcal/mol lower than the barrier for hydrogen abstraction. The calculated ene geometries are unusual for a pericyclic reaction in that hydrogen transfer from **AH** to styrene is clearly occurring but C−C bond formation has progressed very little. Despite the unusual geometry, several features suggest that these TSs do correspond to the ene reaction and not to another possible

conformation for hydrogen abstraction. As compared to the abstraction TSs, the ene transition structures have the following characteristics: (1) they are significantly more stable, indicating that the incipient radical centers are strongly interacting and pericyclic overlap is present, (2) the hydrogen is transferred to styrene to a smaller extent, signifying that they are earlier than the abstraction TSs, and (3) the C--H--C geometry is bent, not linear, which is necessary to maintain cyclic overlap. IRC calculations confirm the concerted nature of the ene TSs; therefore, we conclude that the ene reaction of **AH** and styrene is an important contributor to the formation of trimer **A-Sty** and serves to decrease the concentration of **AH** that can undergo hydrogen abstraction.

Scheme 5

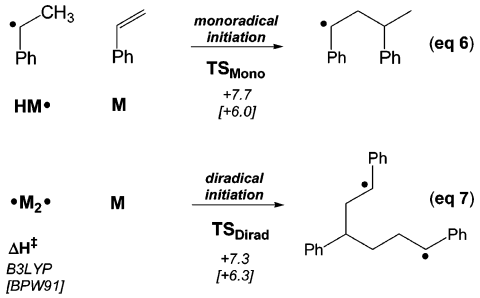

A final consideration is whether a monoradical initiator is inherently superior to a diradical initiator at adding to a monomer. This was examined by comparing $\mathbf{TS_{mono}}$ and $\mathbf{TS_{dirad}}$ (Scheme 5, Figure 11). $\mathbf{TS_{mono}}$ corresponds to the addition of phenylethyl radical to styrene. It has an enthalpic barrier of 6−8 kcal/mol relative to noninteracting styrene and phenylethyl radical. $\mathbf{TS_{dirad}}$ corresponds to the addition of $\mathbf{^{\bullet}M_2^{\bullet}}$ to styrene, and its barrier also falls in the 6−8 kcal/mol range. These results are consistent with the conclusion that diradical chain propagation is not disfavorable because of a high barrier for addition to monomer but because of a high rate of intramolecular self-termination.[3,37] The difference in computed $\Delta G^{\ddagger}$ values predict that self-termination of the 1,4-diradical occurs over 10^{11} times faster than diradical propagation.[38]

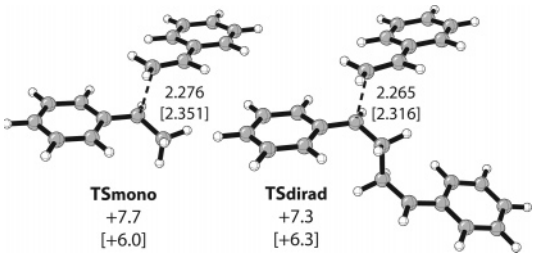

Figure 11. TS models for monoradical and diradical styrene propagation. B3LYP, B3LYP with spin projection (in parentheses), and BPW91 [in brackets] enthalpies in kcal/mol. Bond lengths are given in Å.

Combination of Experimental and Computational Results: The Mechanism for Styrene Self-Initiation. As discussed in the background section, the Mayo mechanism for self-initiated styrene polymerization gains strong support from experimental studies: the trapping experiments, the KIE studies, and the decomposition of azo compounds **4** and **5**. The experimental results point to the key role of the **AH** intermediate and to the inadequacy of the 1,4-diradical in promoting styrene polymerization.

Computationally, the results are not as clear-cut. First, concerted pericyclic transition structures for the formation of **AHx** or **AHn** cannot be located, indicating that styrene dimerization via a concerted Diels−Alder process is more energetically demanding than dimerization via a stepwise diradical process. Second, the 1,4-diradical $\mathbf{^{\bullet}M_2^{\bullet}}$ can ring-close to either the **DCB** or to **AH**, but both experiment and computations agree that the **DCB** dimers should be formed much faster than the **AH** dimers.[39] Third, hydrogen abstraction from **AH** is predicted to be much more facile than hydrogen abstraction from $\mathbf{^{\bullet}M_2^{\bullet}}$. The question now becomes how can a diradical mechanism account for the formation of **AH** at a rate large enough to account for self-initiation and **A-Sty** formation?

Since transition-state theory predicts formation of diphenylcyclobutane will dominate, we were forced to consider the possibility that deviations from transition-state theory might be involved. Carpenter, Doubleday, and others have shown cases where dynamic considerations and deviations from transition-state theory influence products of reaction.[40] We have explored in more detail whether dynamic effects might cause greater amounts of **AH** to be formed than would be expected from transition-state theory.

Scheme 6

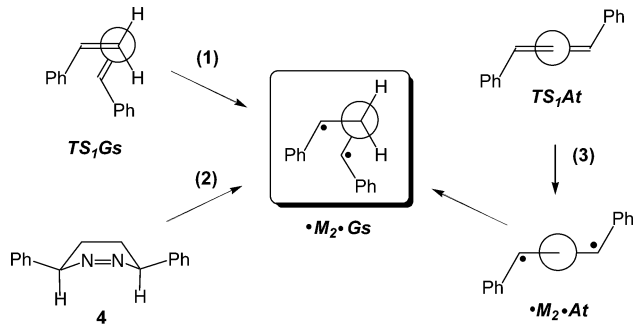

I. An unexpectedly high ratio of **AH** versus **DCB** produced from the 1,4-diradical intermediate can be explained if the reactivity of the 1,4-diradical is influenced by its mechanism of formation. Theoretically, such phenomena will be observed when the rate of intramolecular vibrational energy redistribution of an activated intermediate is slower than the rate of reaction.[40]

For example, the $\mathbf{^{\bullet}M_2^{\bullet}Gs}$ can be formed from at least three distinct reactions (Scheme 6): (1) one-step formation via transition-state $\mathbf{TS_1Gs}$; (2) one-step formation via loss of N_2 from **4**; and (3) multistep formation via transition-state $\mathbf{TS_1Aa}$ followed by rotational transition states. Our hypothesis is that the mode of forming $\mathbf{^{\bullet}M_2^{\bullet}Gs}$ will strongly influence which of the vibrational modes of the 1,4-diradical will have excess energy and thereby influence whether the $\mathbf{^{\bullet}M_2^{\bullet}Gs}$ will ring-

(37) Rule, J. D.; Wilson, S. R.; Moore, J. S. *J. Am. Chem. Soc.* **2003**, *125*, 12992−12993.

(38) $k = \mathrm{kbT/h}\ \exp\wedge(-\Delta G/\mathrm{RT})^{*}(\mathrm{mol/L})^{1-n}$, where n is the order of the reaction. The density of styrene at 20 °C is 0.9059 g/mL, equating to a concentration of 8.7 M. Boyer, R. F.; Keskkula, H.; Platt, A. E. Styrene Polymers. *Encyclopedia of Polymer Science and Technology*, Vol. 13; Wiley & Sons: New York, 1970; p 136.

(39) Transition-state theory predicts that Diels−Alder adducts would compose less than 0.1% (B3LYP) or 1% (BPW91) of the total amount of dimers formed at 180 °C.

(40) Carpenter, B. K. *J. Phys. Org. Chem.* **2003**, *16*, 858−868 and references therein.

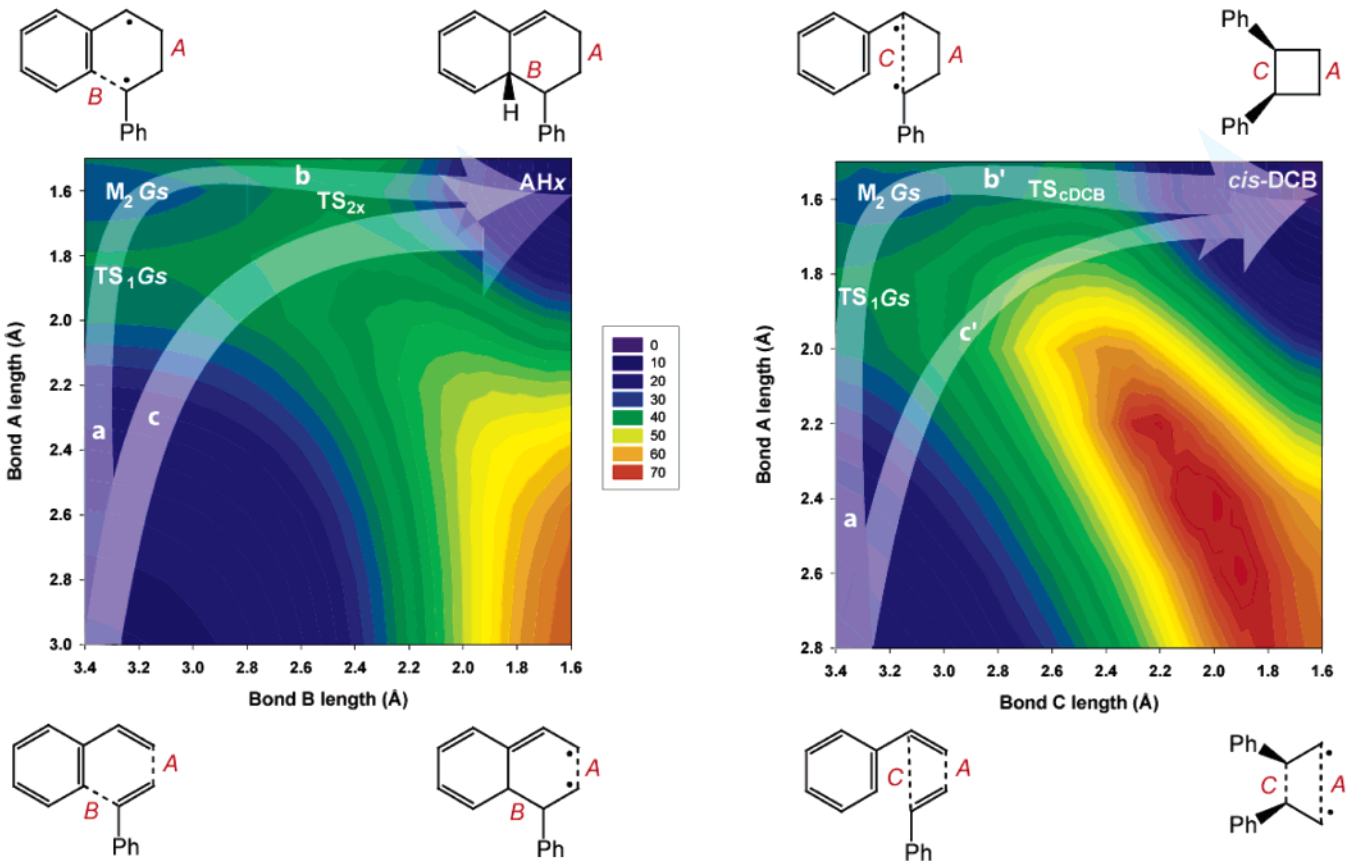

Figure 12. B3LYP contour plots for conversion of two molecules of styrene into **AHx** (plot 1) and to *cis*-**DCB** (plot 2). The lowest energy pathway is denoted by arrows **a**, and in both plots, this pathway involves formation of the diradical intermediate **•M₂•Gs**. Arrow **b** indicates a higher energy pathway accessible by a nonequilibrium dynamic effect that accounts for an increased rate of formation for **AHx**.

close to *cis*-**DCB**, ring-close to **AHx**, cleave to styrene, or undergo additional rotations to generate other **•M₂•** conformers.

The UB3LYP contour energy plots in Figure 12 can be used to illustrate how dynamics might influence the reactivity of **•M₂•Gs**.[41] Plot 1 illustrates the conversion of two molecules of styrene into the **AHx** dimer, whereas plot 2 illustrates conversion into the *cis*-**DCB** dimer. In both plots, motion along the *y*-axis corresponds to formation of bond A, generating the **•M₂•Gs** intermediate. Motion along the *x*-axis corresponds to formation of bond B in plot 1 or bond C in plot 2.

According to the tenets of transition-state theory (TST), the ratio of **AHx** to *cis*-**DCB** is governed only by the relative barriers heights of $\mathbf{TS_{2x}}$ and $\mathbf{TS_{cDCB}}$. When **•M₂•Gs** occupies a vibrational ground state (e.g., there is no "memory" for how the diradical was formed), TST would predict that *cis*-**DCB** (pathway **b′**) would be produced 60 times (based on $\Delta\Delta H^{\ddagger}$) faster than **AHx** (pathway **b**). However, if **•M₂•Gs** is generated with a nonstatistical distribution of vibrational energy, the rate of formation of **AHx** relative to *cis*-**DCB** would be altered. We predict that reaction 1, single-step formation of the 1,4-diradical via $\mathbf{TS_1Gs}$, is responsible for an enhanced rate of formation of **AHx**. This transition structure is more similar to $\mathbf{TS_{2x}}$ than to $\mathbf{TS_{cDCB}}$ in structure and would therefore be more likely to excite the vibrations leading to **AHx** than to *cis*-**DCB**. The dynamic control would lead to the preference of pathway **ab** over **ab′**. For such an effect to be operative, the lifetime of the 1,4-diradical must be extremely short, effectively making the two-step diradical process into a two-phase, single-step process analogous to a concerted, if highly asynchronous, Diels−Alder reaction.

Other mechanisms that generate **•M₂•Gs**, either $\mathbf{TS_1At}$ followed by various rotational transition states or by thermolysis of compound **4**, are expected to produce the diradical without any predilection to favor the conversion of the 1,4-diradical into **AHx**.

II. Enhanced formation of **AHx** could also be due to dynamic effects prior to the formation of the 1,4-diradical intermediate. The concerted pathway (**c**) in Figures 12 and 13 is only slightly higher in energy than the diradical pathway (**a**) and, therefore, is still thermally accessible. In this scenario, two molecules of styrene approach in the **Gs** orientation, bond A and bond B form in a concerted but very asynchronous fashion such that the system never reaches the **•M₂•Gs** energy well. On the other hand, concerted formation of bonds A and C corresponds to a [2+2] cycloaddition (pathway **c′**) and is prohibitively high in energy. Consequently, a dynamic effect that bypasses formation of **•M₂•Gs** also increases the rate of formation of **AHx** relative to *cis*-**DCB**.

The energy differences between trajectories **a**, **c**, and **c′** are best illustrated in Figure 13, a side-view of the contour surfaces in Figure 12. The [2+2] pathway **c′** is ∼20 kcal/mol higher in energy than [4+2] pathway **c**. The [4+2] pathway **c** is <1 kcal/mol[42] higher in energy than the diradical pathway **a**.

(41) Contour energy surfaces were also generated with R and UBPW91. They show the same general features as the plots in Figures 6 and 7.

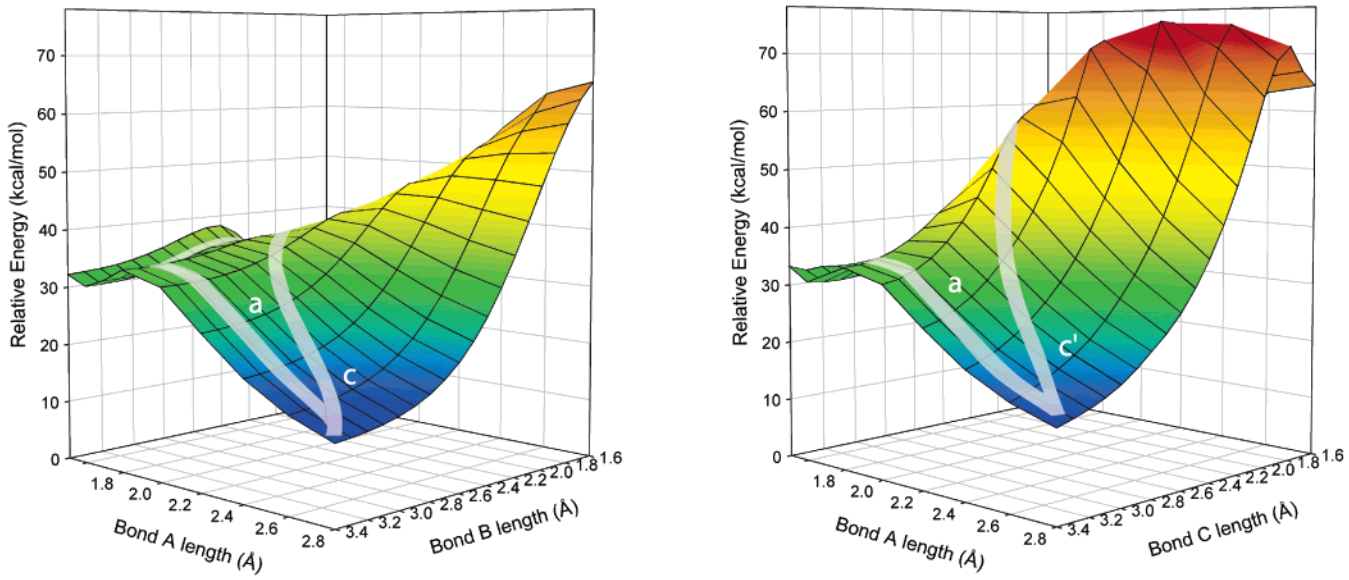

Figure 13. Side-view of the contour surfaces in Figure 12. Plot 1 depicts the formation of **AHx** and plot 2 depicts the formation of *cis*-**DCB**. Pathway **a** corresponds to diradical formation of **•M$_2$•Gs**, pathway **c** to a concerted [4+2], and **c′** to a [2+2] cycloaddition.

Presumably, the dynamic effects described above are two extremes of the same phenomenon: initial trajectories of two styrene molecules in the **Gs** conformation are closely related to a Diels−Alder pathway, such that the shorter the lifetime of the **•M$_2$•Gs** intermediate, the more likely **AHx** will be the preferred cycloadduct. Analogous dynamic effects should also be possible for styrene molecules in the **Gu** conformation, where now the rate of **AHn** formation could be enhanced relative to the rate of *trans*-**DCB** formation. However, the energy differences between pathways to form **AHn** versus *trans*-**DCB** are larger than the energy differences between pathways to form **AHx** versus *cis*-**DCB**; therefore, we would predict that the dynamic rate enhancement of **AHn** formation is less effective.

Scheme 7

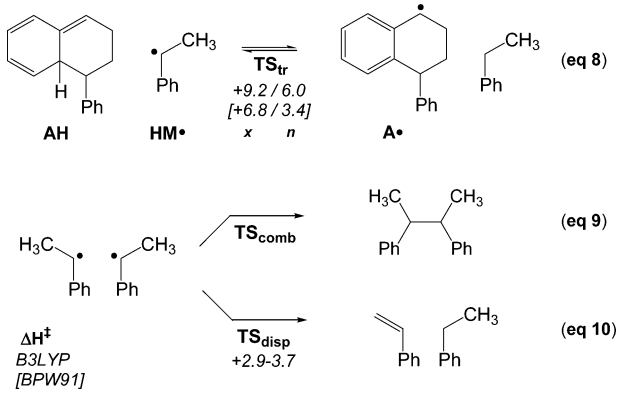

Chain Transfer and Disproportionation. In the previous sections, we focused on the process of initiation and briefly touched on propagation. Here, we will briefly discuss chain transfer and termination, the two remaining processes involved in styrene polymerization (Scheme 7). Model reactions were calculated for comparison to the experimental rates (Table 2, Figure 14).

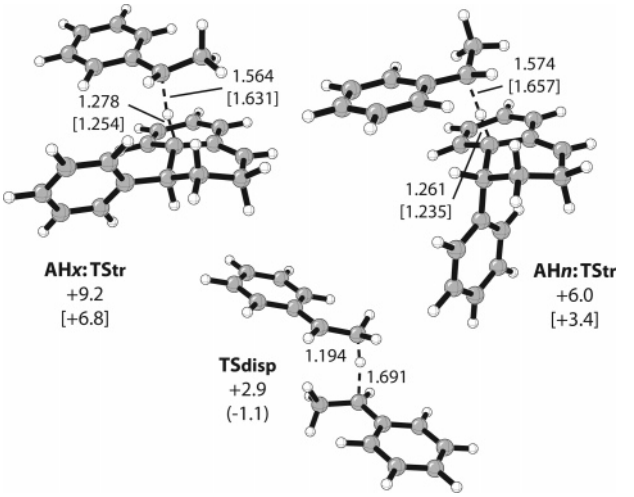

Figure 14. TSs for chain transfer from phenylethyl radical **HM•** to **AH**. Disproportionation TS of two phenylethyl radicals. B3LYP, B3LYP with spin projection (in parentheses), and BPW91 [in brackets] enthalpies in kcal/mol. Bond lengths are given in Å.

Chain transfer is a reaction in which a growing polymer radical abstracts an atom from a chain-transfer agent to produce a "dead" polymer and a new radical. If the new radical is reactive enough to reinitiate a new polymer chain, then the chain transfer has no effect on the rate of polymerization, and it reduces the molecular weight of the polymer. The efficiency of transfer is measured by a chain-transfer constant (*C*) which is the ratio of the transfer rate to the propagation rate.[43]

Chain transfer to **AH** can account for the observed changes in molecular weight of polystyrene as a function of percent conversion.[3,44] At very low conversions, extremely high molecular weight polymer is obtained because of the low concentration of **AH**, whereas at higher conversions, the molecular

(42) The UB3LYP/6-31G* energy (no ZPE) of the **TS$_1$Gs** is −619.256742 au. The UB3LYP/6-31G* single-point energy (no ZPE) of the concerted transition structure **AHx**−**TS$_{DA}$** is −619.255546 au.

(43) (a) Boyer, R. F.; Keskkula, H.; Platt, A. E. Styrene Polymers. In *Encyclopedia of Polymer Science and Technology*; Wiley & Sons: New York, 1970; 13, pp 173−175. (b) Mayo, F. R. *J. Am. Chem. Soc.* **1943**, *65*, 2324−2329.

(44) (a) Lebovits, A.; Teach, W. C. *J. Polym. Sci.* **1960**, *47*, 527−529. (b) Louchex, C.; Benoit, H. *Compt. Rend.* **1960**, *251*, 382−384. (c) Müller, K. F. *Makromol. Chem.* **1964**, *79*, 128−134.

weight decreases and then plateaus as the **AH** concentration reaches its steady state. Knowing the activation energy for transfer of ethylbenzene is 12.8 kcal/mol[45] and assuming the transfer constant for **AH** is 1,[46] Pryor and Lasswell estimates the activation energy for transfer to **AH** to be 6.7 kcal/mol.[3] B3LYP calculations on a model system, chain transfer from phenylethyl radical (eq 8) to **AHn** or **AHx**, predict that transfer has an activation enthalpy of ~6 kcal/mol and ~9 kcal/mol, respectively. The process of termination was modeled computationally with the combination and disproportionation of two phenylethyl radicals (eqs 9 and 10, respectively). A transition structure for combination could not be located using either B3LYP or BPW91 because there is no enthalpic barrier for σ-bond formation. However, a barrier on the free-energy surface would exist because the entropy decreases when the two radical species are brought together in the proper orientation. Transition structures for disproportionation were located with B3LYP; activation enthalpies of ~3−4 kcal/mol are found for this reaction in different conformations. The calculations are in reasonable agreement with the experimental ΔH_{298K} value of 2.2 kcal/mol.[28]

Conclusion

B3LYP/6-31G(d) and BPW91/6-31G(d) confirm that **AH**, the Diels−Alder styrene dimer, is the key intermediate for self-initiation of styrene polymerization. Scheme 8 summarizes our current understanding of the mechanism for styrene self-initiation, and the reactions highlighted in gray are necessary steps in the thermal polymerization.

Scheme 8

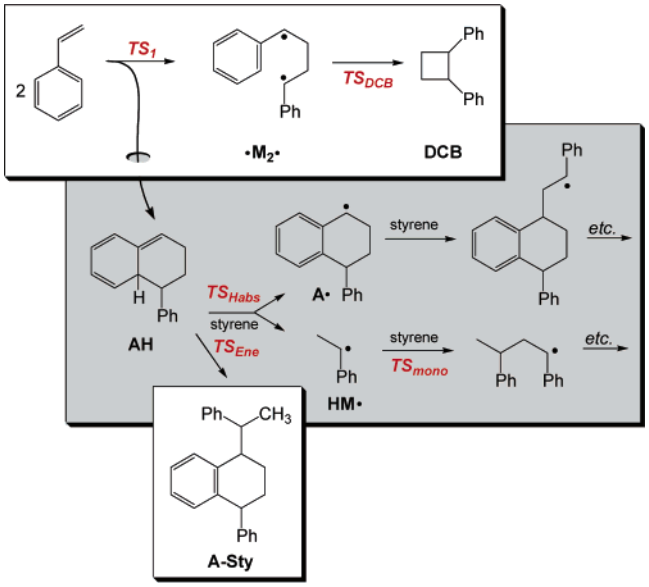

The lowest energy pathway for reaction of two molecules of styrene is formation of the 1,4-diradical **•M$_2$•** via **TS$_1$**, and the barrier ($\Delta H^{\ddagger}_{B3LYP}$) for this reaction ranges from 25 to 27 kcal/mol, depending on the conformation in which the two molecules of styrene approach each other. Although the 1,4-diradical can adopt numerous anti and gauche conformations that are essentially isoenergetic (ΔH_{B3LYP} = 20−21 kcal/mol), the lifetime of the diradical is too short to achieve complete conformational equilibration or to react with a third molecule of styrene. Consequently, the diradical **•M$_2$•** is unable to undergo hydrogen abstraction (to product monoradicals) or propagation (to produce a growing polystyryl diradical). In the absence of any dynamic effects, the gauche 1,4-diradical undergoes very fast ring closure to **DCB**, effectively terminating the polymerization before it ever starts; the barrier ($\Delta H^{\ddagger}_{B3LYP}$) for closure to *cis*-**DCB** is only +2.6 kcal/mol and the barrier to *trans*-**DCB** is even lower.

We predict that dynamic effects mirroring the concerted Diels−Alder pathway can override the very fast formation of **DCB** such that **AH** is formed at the expense of **DCB**. In the absence of additional styrene monomer, it is likely that the **AH** would revert to the diradical intermediate. However, in the presence of styrene, a third monomer can abstract hydrogen from **AH** via several possible conformations of **TS$_{Habs}$** ($\Delta H^{\ddagger}_{B3LYP}$ = 23−24 kcal/mol), generating two benzylic monoradicals. The calculated free energies indicate that the abstraction is the rate-determining step, which corresponds to a third-order initiation. Both monoradicals **A•** and **HM•** are responsible for initiating polymerization, and the calculated barrier for propagation (**TS$_{mono}$**) is ~7 kcal/mol.

AH can also undergo an ene reaction with styrene to generate inactive trimer **A-Sty**. The barrier **TS$_{Ene}$** is lower than **TS$_{Habs}$**. This is a reasonable prediction because the trimer component formed during polymerization is ~10 times larger than either the dimer or polymer component (see Table 1). Finally, **AH** can serve as a chain-transfer agent with a growing polystyrene chain. The facile transfer reaction simultaneously produces a dead polystyrene chain and generates additional initiator **A•**.

In general, B3LYP predicts higher barriers for the transition structures and deeper wells for the diradical intermediates. Experimental activation parameters are available for formation and disappearance of **DCB**, and B3LYP shows better agreement than BPW91 with these values.

Acknowledgment. We thank Prof. Roderic Quirk for many helpful discussions. We are grateful to the National Science Foundation for financial support of this research through a research grant to K.N.H. and a graduate fellowship to K.S.K.. We also thank the National Computational Science Alliance under grant MCA93S015N and the UCLA Office of Academic Computing for computational resources.

Supporting Information Available: B3LYP/6-31G(d) and BPW91/6-31G(d) Cartesian coordinates, electronic energies, enthalpies, free energies, and entropies for all stationary points. Imaginary frequencies and $\langle S^2 \rangle$ values for entries in Table 3 are also included. This material is available free of charge via the Internet at http://pubs.acs.org.

JA0448667

(45) Gregg, R. A.; Mayo, F. R. *Discuss. Faraday Soc.* **1947**, *2*, 328−337.
(46) Pryor, W. A.; Coco, J. H. *Macromolecules* **1970**, *3*, 500−508.